Inorg. Chem. **2008**, *47*, 49–55

Bluish-White Emission from Radical Carbonyl Impurities in Amorphous Al_2O_3 Prepared via the Pechini-Type Sol–Gel Process

Cuikun Lin, Min Yu, Ziyong Cheng, Cuimiao Zhang, Qingguo Meng, and Jun Lin*

State Key Laboratory of Application of Rare Earth Resources, Changchun Institute of Applied Chemistry, Chinese Academy of Sciences, Changchun 130022, People's Republic of China

Received April 5, 2007

Many efforts have been devoted to exploring novel luminescent materials that do not contain expensive or toxic elements, or do not need mercury vapor plasma as the excitation source. In this paper, amorphous Al_2O_3 powder samples were prepared via the Pechini-type sol–gel process. The resulting samples were characterized by X-ray diffraction (XRD), Fourier transform infrared (FT-IR) spectroscopy, field emission scanning electron microscopy (FESEM), photoluminescence (PL) excitation and emission spectra, kinetic decay, and electron paramagnetic resonance (EPR). The obtained amorphous Al_2O_3 powder samples annealed at 500 and 600 °C exhibit bright bluish-white emission centered at 430 and 407 nm, respectively. The luminescent mechanisms of the amorphous Al_2O_3 powder samples can be ascribed to the carbon-related impurities such as radical carbonyl species. The calculated band structure of the defective amorphous Al_2O_3 agrees well with the results of spectral analysis and the proposed luminescent mechanism.

I. Introduction

Luminescent materials play an important role in modern society for information displays and lighting.[1,2] Most of the commercial lamp phosphors require excitation by short ultraviolet (UV) light for operation, such as mercury vapor plasma in fluorescent lighting products.[3] In addition, the activators in fluorescent lamp or cathodoluminescent display phosphors are often expensive or toxic elements.[1−3] Therefore, much effort has been devoted to exploring novel luminescent materials which do not contain expensive or toxic elements[4−9] or do not need mercury vapor plasma as the excitation source.[2,10]

The Pechini-type sol−gel process (also known as the polymerizable-complex technique), is well-known and is extensively used for the synthesis of homogeneous (especially multicomponent) metal oxide materials.[11] This method has been used for the synthesis of electric and magnetic materials rather extensively, including ferroelectric and capacitor materials, superconducting materials, and photocatalytic materials.[11] The improved material properties for the Pechini-type sol−gel process with respect to other methods (such as the solid-state reaction method and amorphous citrate method) have been demonstrated for the synthesis of superconductors and photocatalysts.[11c] In the past five years, we have extended the application of the Pechini-type sol−gel process to the systematic synthesis of various kinds of optical materials, including luminescent powders and thin films, core−shell structured phosphor, and pigment materials.[12]

Alumina is an important material for the ceramic industry. Amorphous Al_2O_3 has found extensive application in catalysis, coatings, microelectronics, and thin film devices.[13−18]

* To whom correspondence should be addressed. E-mail: jlin@ciac.jl.cn.

(1) Blasse, G.; Grabmaier, B. C. *Luminescent Materials*; Springer-Verlag: Berlin, 1994.
(2) Feldmann, C.; Jüstel, T.; Ronda, C. R.; Schmidt, P. J. *Adv. Funct. Mater.* **2003**, *13*, 511.
(3) Ropp, R. C. *Luminescence and the Solid State*; Elsevier: Amsterdam, Netherlands, 1991; Vol. 12, p 283.
(4) Green, W. H.; Le, K. P.; Grey, J.; Au, T. T.; Sailor, M. J. *Science* **1997**, *276*, 1826.
(5) Hayakawa, T.; Hiramitsu, A.; Nogami, M. *Appl. Phys. Lett.* **2003**, *82*, 2975.
(6) (a) Brankova, T.; Bekiari, V.; Lianos, P. *Chem. Mater.* **2003**, *15*, 1855. (b) Bekiari, V.; Lianos, P. *Langmuir* **1998**, *14*, 3459.
(7) Yold, B. E. *J. Non-Cryst. Solids* **1992**, *147*, 614.
(8) (a) Carlos, L. D.; Sá Ferreira, R. A.; Pereira, R. N.; Assuncão, M.; de Zea Bermudez, V. *J. Phys. Chem. B* **2004**, *108*, 14924. (b) Fu, L.; Sá Ferreira, R. A.; Silva, N. J. O.; Carlos, L. D.; de Zea Bermudez, V.; Rocha, J. *Chem. Mater.* **2004**, *16*, 1507. (c) Carlos, L. D.; de Zea Bermudez, V.; Sá Ferreira, R. A.; Marques, L.; Assunção, M. *Chem. Mater.* **1999**, *11*, 581.
(9) Lin, J.; Baerner, K. *Mater. Lett.* **2000**, *46*, 86.
(10) Wegh, R. T.; Donker, H.; Oskam, K. D.; Meijerink, A. *Science* **1999**, *283*, 663.
(11) (a) Pechini, M. P. U.S. Patent 3,330,697, 1967. (b) Kakihana, M.; Yoshimura, M. *Bull. Chem. Soc. Jpn.* **1999**, *72*, 1427. (c) Kakihana, M.; Domen, K. *MRS Bull.* **2000**, *25* (9), 27.

10.1021/ic700652v CCC: $40.75
Published on Web 12/11/2007

The photoluminescence properties in porous alumina membrane have been paid much attention in the past decade.[19−21] Zhang and coauthors reported on blue luminescence from alumina nanoparticles suspended in toluene solution through ultrasonic treatment of a porous anodic alumina membrane.[21a] Mohanty etc. dispersed Eu_2O_3 nanoparticles in amorphous Al_2O_3 to enhance the photoluminescence.[21c] However, so far little attention has been paid to the emission properties in this material prepared by the Pechini-type sol−gel process.

It has been reported that sol−gel derived SiO_2-based materials, including SiO_2 gels and organic/inorganic hybrid silicones, show strong luminescence from the blue to red spectral region. These materials are potentially used as a kind of environmentally friendly luminescent material without expensive or toxic metal elements as activators.[8] Recently, we found that Pechini-type sol−gel derived BPO_4 doped with Ba^{2+} emits an efficient bluish-white light.[12b] Nanocrystalline tetragonal ZrO_2 powders prepared by the Pechini-type sol−gel method also show a strong bluish-white emission. The luminescence mechanism of nanocrystalline ZrO_2 can be ascribed to the interstitial carbon defects (C_i) in tetragonal ZrO_2.[12e]

Considering the above situations, it would be of great interest and importance to check if such strong emission can be observed in other oxide systems prepared by a similar process. Furthermore, it would be possible to find some useful luminescent materials via such an investigation. Accordingly, in this paper we prepared amorphous Al_2O_3 samples via the Pechini-type sol−gel process. It is interesting to find that this material also shows an intense bluish-white emission (λ_{max} = 407−430 nm) under a wide range of UV light excitation (230−420 nm). Possible mechanisms have been proposed to explain the observed luminescent phenomena.

II. Experimental Section

Preparation. Al_2O_3 powder samples were prepared via the Pechini-type sol−gel method (SG).[11,12] Typically, 1.88 g of $Al(NO_3)_3 \cdot 9H_2O$ (A. R., Beijing Beihua Chemicals Co., Ltd.) was dissolved in an aqueous solution under vigorous stirring, and then mixed with a 40 mL water−glycerol (v:v = 1:7) solution containing citric acid (A. R., Beijing Beihua Chemicals Co., Ltd.) as the chelating agent for the metal ions. The molar ratio of the metal ions to citric acid was 1:2. A 4.00 g sample of poly(ethylene glycol) (PEG, 20000; A. R., Beijing Beihua Chemicals Co., Ltd.) was added as a cross-linking agent. The solution was stirred for 1 h to form a sol, and then the sample was immediately dried at 150 °C for 6 h. The obtained precursor material was preheated at 400 °C for 3 h, was fully ground, and was sintered at the desired temperature (500−900 °C) in air for 3 h to produce the final sample. As a comparison with the samples prepared via the Pechini-type sol−gel process, 3.00 g of $Al(NO_3)_3 \cdot 9H_2O$ was annealed directly at 500 °C in air for 3 h to obtain Al_2O_3 (solid-state process, SS) powder sample. We denote the final samples as follows. AOSG*x* series (*x* = 500, 600, 700, 800, and 900) denotes the Al_2O_3 samples prepared via the Pechini-type sol−gel process, where *x* is the annealing temperature (°C). AOSS500 stands for the sample obtained by the solid-state reaction, and here 500 denotes the annealing temperature (500 °C).

Characterization. The X-ray diffraction (XRD) of powder samples was examined on a Rigaku-Dmax 2500 diffractometer using Cu Kα radiation (λ = 0.15405 nm). Fourier transform infrared (FT-IR) spectra were measured with a Perkin-Elmer 580B infrared spectrophotometer with the KBr pellet technique. The morphology and composition of the samples were inspected using a field emission scanning electron microscope (FESEM; XL30, Philips) equipped with an energy-dispersive X-ray spectrometer (EDS; JEOL JXA-840). The excitation and emission spectra were taken on a Hitachi F-4500 spectrofluorimeter equipped with a 150 W xenon lamp as the excitation source. Luminescence lifetimes were measured with a Lecroy Wave Runner 6100 digital oscilloscope (1 GHz) using 280 nm lasers (pulse width = 4 ns) as the excitation source (Continuum Sunlite OPO). Electron paramagnetic resonance (EPR) spectra were taken on the JESFE3AX electronic spin resonance spectrophotometer. All the measurements were performed at room temperature. The band structures of the defective amorphous Al_2O_3 were calculated using the CASTEP code (version 3.0, Accelrys) based on the density functional theory (DFT).

III. Results and Discussion

XRD and FT-IR. The XRD patterns of Al_2O_3 samples prepared by the Pechini-type sol−gel process and solid-state reaction are shown in Figure S1: (a) AOSS500, (b) AOSG500, (c) AOSG600, (d) AOSG700, (e) AOSG800, and (f) AOSG900, respectively (Supporting Information). Only amorphous materials were produced at lower temperatures (500−600 °C), as shown in Figure S1 (a−c).[22] For the samples annealed at 800 and 900 °C, diffraction peaks at 37.6, 45.8, and 67.6° are present, which belong to (311), (400), and (440) reflections of η-Al_2O_3 (JCPDS Card No. 77-0396). No other phase was detected, indicating that phase transformation from amorphous Al_2O_3 to η-Al_2O_3 begins to take place around 800 °C.

(12) (a) Yu, M.; Lin, J.; Fang, J. *Chem. Mater.* **2005**, *17*, 1783. (b) Lin, C. K.; Luo, Y.; You, H.; Quan, Z.; Zhang, J.; Fang, J.; Lin, J. *Chem. Mater.* **2006**, *18*, 458. (c) Yu, M.; Lin, J.; Wang, Z.; Fu, J.; Wang, S.; Zhang, H. J.; Han, Y. C. *Chem. Mater.* **2002**, *14*, 2224. (d) Wang, H.; Lin, C. K.; Liu, X. M.; Lin, J.; Yu, M. *Appl. Phys. Lett.* **2005**, *87*, 181907. (e) Lin, C. K.; Zhang, C. M.; Lin, J. *J. Phys. Chem. C* **2007**, *111*, 3300.

(13) (a) Costina, I.; Franchy, R. *Appl. Phys. Lett.* **2001**, *78*, 4139. (b) Hou, Y. J.; Wang, Y. Q.; He, F.; Mi, W. L.; Li, Z. H.; Wu, W.; Min, E. Z. *Appl. Catal., A* **2004**, *259*, 35. (c) Myung, S. T.; Izumi, K.; Komaba, S.; Sun, Y. K.; Yashiro, H.; Kumagai, N. *Chem. Mater.* **2005**, *17*, 3695.

(14) (a) Stoloff, N. S.; Liu, C. T.; Deevi, S. C. *Intermetallics* **2000**, *8*, 1313. (b) Chang, H.; Choi, Y.; Kong, K.; Ryu, B. H. *Chem. Phys. Lett.* **2004**, *391*, 293.

(15) Jimenéz-Gonzales, A.; Schmeisser, D. *Surf. Sci.* **1991**, *250*, 59.

(16) Ealet, B.; Elyakhloufi, M. H.; Gillet, E.; Ricci, M. *Thin Solid Films* **1994**, *250*, 92.

(17) Gautier, M.; Duraud, J. P.; Van, L. P.; Guittet, M. J. *Surf. Sci.* **1991**, *250*, 71.

(18) Bianconi, A.; Bachrach, R. Z.; Hagstrom, S. H.; Flodström, S. A. *Phys. Rev. B* **1979**, *19*, 2837.

(19) Du, Y.; Cai, W. L.; Mo, C. M.; Chen, J.; Zhang, L. D.; Zhu, X. G. *Appl. Phys. Lett.* **1999**, *74*, 2951.

(20) Huang, G. S.; Wu, X. L.; Mei, Y. F.; Shao, X. F.; Siu, G. G. *J. Appl. Phys.* **2003**, *93*, 582.

(21) (a) Zhang, W. J.; Wu, X. L.; Fan, J. Y.; Huang, G. S.; Qiu, T.; Chu, P. K. *J. Phys: Condens. Matter* **2006**, *18*, 9937. (b) Chen, J. H.; Huang, C. P.; Chao, C. G.; Chen, T. M. *Appl. Phys. A: Mater. Sci. Process.* **2006**, *84*, 297. (c) Mohanty, P.; Ram, S. *J. Mater. Chem.* **2003**, *13* (12), 3021−3025.

(22) (a) Liu, M.; Li, H.; Xiao, L.; Yu, W.; Lu, Y.; Zhao, Z. *J. Magn. Magn. Mater.* **2005**, *294*, 294. (b) Hung, P. K.; Vinh, L. T. *J. Non-Cryst. Solids* **2006**, *352*, 5531.

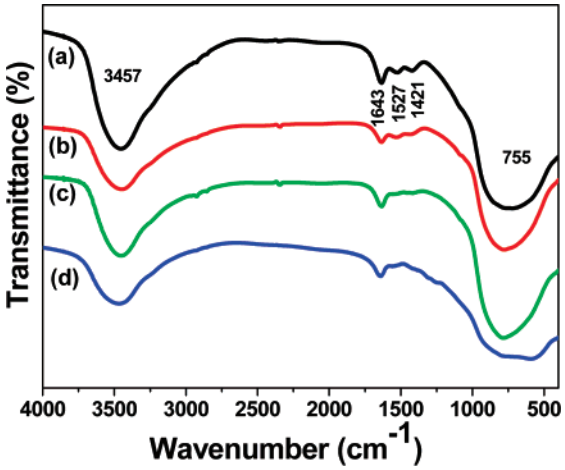

Figure 1. FT-IR spectra of Al_2O_3 prepared by Pechini-type sol−gel process (SG) and solid-state reaction (SS). (a) AOSG500, (b) AOSG600, (c) AOSG700, and (d) AOSS500.

The FT-IR spectra of Al_2O_3 prepared by the Pechini-type sol−gel process and solid-state reaction are shown in Figure 1 (a) AOSG500, (b) AOSG600, (c) AOSG700, and (d) AOSS500, respectively. The band at 3457 cm^{-1} is due to the stretching mode of hydroxyl groups (from surface water and adsorbed water), and the band at 1643 cm^{-1} is due to the bending mode of water molecules. The broad band at 755 cm^{-1} can be ascribed to the Al−O vibration of (AlO_4).[5,23] The weak bands at 1435 and 1527 cm^{-1} can be ascribed to the stretching vibrations of carboxylate groups,[12b,e,23] indicating that the carbon impurity has not been removed completely in the Pechini-type sol−gel derived samples due to the fact that they have been annealed at relatively low temperature (500 °C). The carbon impurity can also be detected by energy-dispersive X-ray spectroscopy for the AOSG500 (EDS; see next section).

FESEM and EDS. Figure 2 shows the FESEM image (a) and the energy-dispersive X-ray spectrum (EDS) (b) of the AOSG500 sample, respectively. From Figure 3a, we can see that the Al_2O_3 (AOSG500) sample is porous, with pore sizes ranging from 50 to 150 nm in diameter. The EDS examination confirms the presence of Al and O from the sample, Si from the Si substrate, and Au from the coating for SEM measurement. The detected carbon impurity (C, also observed in the IR spectra) is from the sample prepared by the Pechini-type sol−gel process, in which some organic solvents and additives (glycerol and PEG) were employed.

Photoluminescence Properties. The AOSG500, AOSG600, AOSG700, and AOSS500 samples exhibit brown, near-white, white, and yellow color under sunlight, respectively. Under UV-lighting excitation, the AOSS500 samples show no luminescence, while the AOSG500, AOSG600, and AOSG700 samples exhibit bluish-white and weak blue luminescence, respectively.

Figure 3 shows the excitation (a) and emission (b) spectra of AOSG500, AOSG600, AOSG700, and AOSS500 samples, respectively. For AOSS500, the excitation and emission

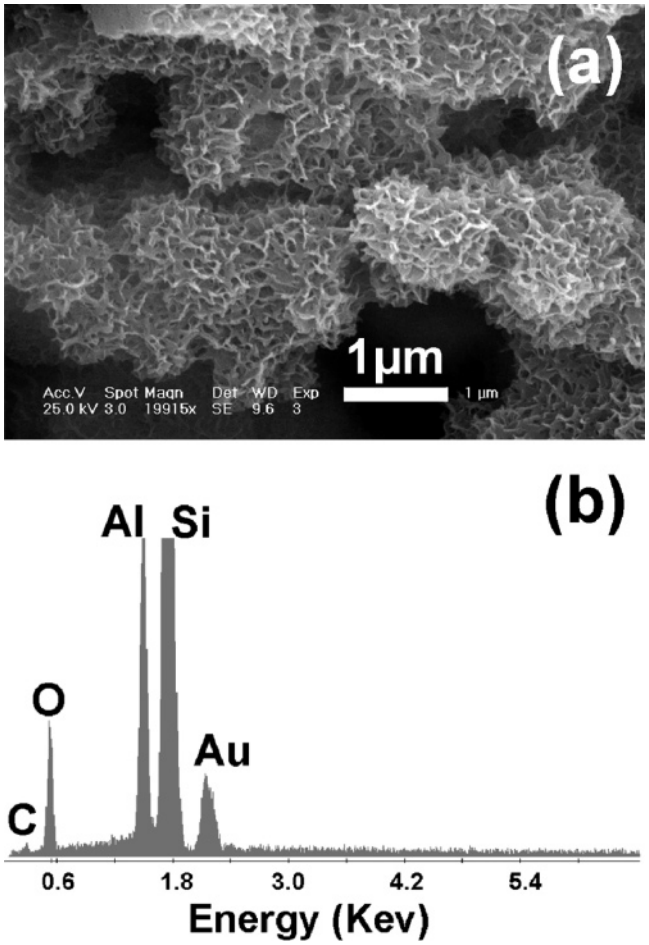

Figure 2. (a) FESEM micrograph and (b) EDS of AOSG500 sample.

spectra cannot be detected (Figure 3, blue line). The luminescence spectra of the AOSG800 and AOSG900 samples cannot be detected either and will not shown here. For AOSG500, the sample shows a strong emission band ranging from 350 to 600 nm, peaking from 407 to 450 nm (centered at 430 nm) (Figure 3b, black lines). The corresponding excitation spectrum includes a broad band from 235 to 425 nm (Figure 3a, black line). The emission spectrum of AOSG600 sample exhibits luminescent properties similar to those of AOSG500 except for the emission intensity. Its emission spectrum also consists of a strong broad band ranging from 350 to 600 nm with a maximum at 407 nm (Figure 3b, red line), whose integrated intensity is enhanced 4 times with respect to that of AOSG500. The AOSG700 sample also shows a similar emission with a maximum at 386 nm (Figure 3b, green line) except a decrease of the intensity, indicating that the optimal annealing temperature is 600 °C.

The luminescence decay curves for AOSG500, AOSG600, and AOSG700 are shown in Figure 4, parts a, b, and c, respectively. These decay curves can be fitted to a single-exponential function as $I = I_0 \exp(-t/\tau)$ (τ is lifetime), from which the lifetimes are determined to be 6.93, 5.82, and 5.64 ns for AOSG500, AOSG600, and AOSG700, respectively.[24]

(23) Dean, J. A. *Lange's Handbook of Chemistry* (Chinese version); Scientific Publisher of China: Beijing, 2003.

(24) Lin, C. K.; Wang, H.; Kong D. Y.; Yu, M.; Liu, X. M.; Wang, Z. L.; Lin, J. *Eur. J. Inorg. Chem.* **2006**, *18*, 3667.

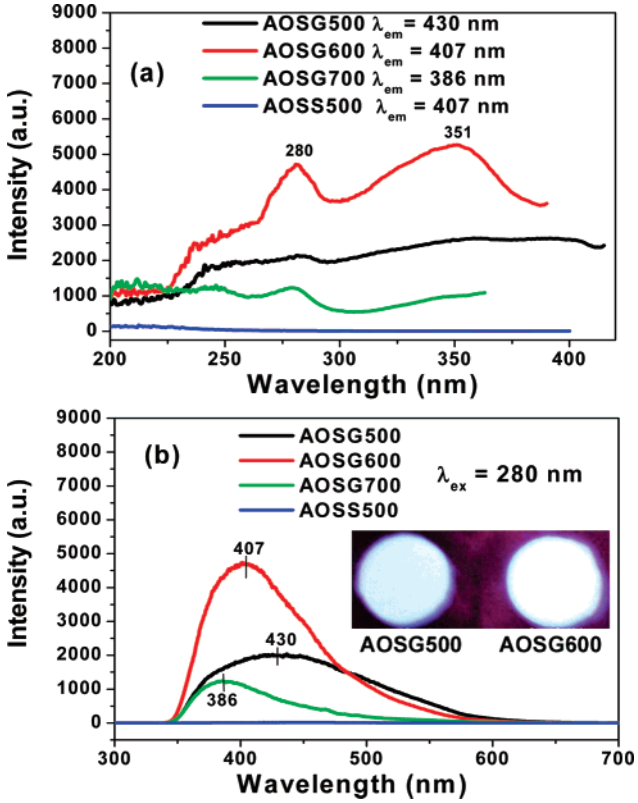

Figure 3. (a) Excitation and (b) emission spectra for AOSG500 (black line), AOSG600 (red line), AOSG700 (green line), and AOSS500 (blue line). The inset of (b) is the luminescent photograph of AOSG500 and AOSG600 under the excitation of a 365 nm UV lamp.

Note that the lifetime deceases a little with the increase of the annealing temperature.

Possible Luminescence Mechanism. Because Al^{3+} itself is not able to show luminescence, the observed luminescence from Al_2O_3 (SG) must be related to some impurities and/or defects in the host lattice, which can be confirmed by the short lifetimes: 6.93, 5.82, and 5.64 ns for AOSG500, AOSG600, and AOSG700, typical values for the luminescence caused by defects.[25,26] The amorphous Al_2O_3 is built up by $(AlO_4)^{5-}$ tetrahedra with corner sharing of oxygen atoms, like the SiO_4 tetrahedral framework in amorphous SiO_2 (including SiO_2 glass,[4,5,7] SiO_2 gels,[4,9] organic/inorganic hybrid silicones,[6,8] silica nanotubes,[27] etc.), all of which are well-known to show luminescence from the blue to the red spectral region. Moreover, molecular sieves such as MCM-41 and MCM-48, open-framework phosphates and germinates, and porous zinc gallophosphates show excellent and tunable luminescence properties in the visible region.[28−31] In all of the above materials, the origins of the luminescence have been ascribed to defects and/ or impurities in the hosts

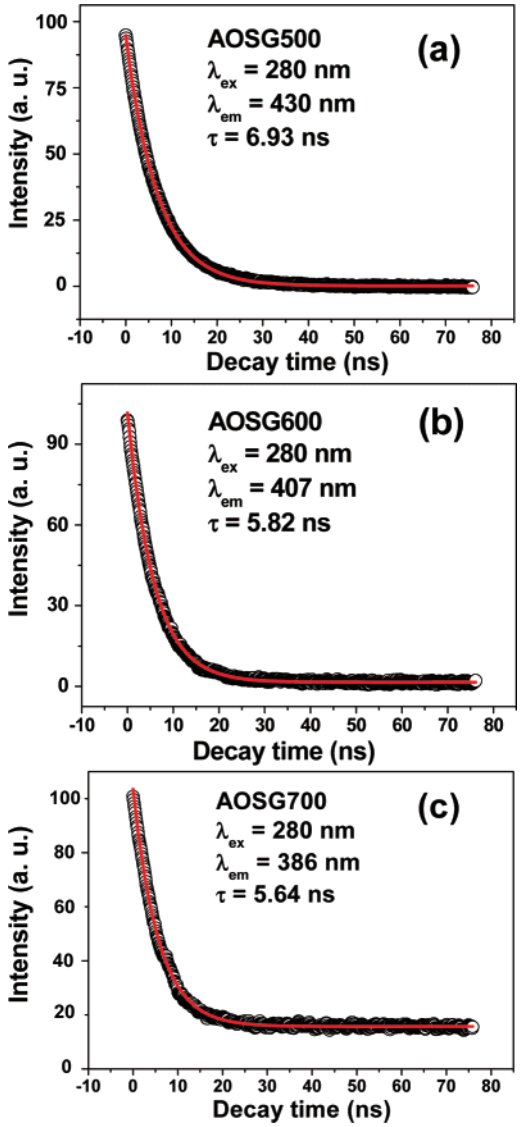

Figure 4. Decay curves for the luminescence of Pechini-type sol−gel derived Al_2O_3: (a) AOSG500, (b) AOSG600, and (c) AOSG700.

without a clear or exact identification of emission centers. For room-temperature-obtained organic/inorganic hybrid silicones containing $-NH_2$ (or $-NH$) groups, Carlos et al. proposed a mechanism based on NH_3^+/NH^- (or NH_2^+/N^-) donor−acceptor pairs to explain the blue emission from these materials.[8] Du et al. ascribed the blue luminescence of alumina membranes with ordered pore arrays to the singly ionized oxygen vacancies (F^+ centers).[19] Hayakawa et al. ascribed the white light emission in $Al_2O_3-SiO_2$ glasses to the radical carbonyl terminations on the surface of pores.[5] Another defect type associated with carbon impurities was proposed as being the origin of the luminescence of sol−gel derived silica gels based on tetraethyl orthosilicate (TEOS) and tetramethoxysilane (TMOS) incorporating a variety of carboxylic acids.[4] Under adequate heat treatments (at least above 247 °C) a carbon impurity is created in the −O−Si−O− network forming −O−C−O− and/or −Si−C− bonds. The carbon-related defects are luminescent active only after a heat treatment because these xerogels are not luminescent prior to this procedure.[8]

(25) Fujimaki, M.; Ohki, Y.; Nishikawa, H. *J. Appl. Phys.* **1997**, *81*, 1042.
(26) Pifferi, A.; Taroni, P.; Torricelli, A.; Valentini, G.; Mutti, P.; Ghislotti, G.; Zanghieri, L. *Appl. Phys. Lett.* **1997**, *70*, 348.
(27) Jang, J.; Yoon, H. *Adv. Mater.* **2004**, *16*, 799.
(28) Gimon-Kinsel, M. E.; Groothuis, K.; Balkus, K. J., Jr. *Microporous Mesoporous Mater.* **1998**, *20*, 67.
(29) Lee, Y. C.; Liu, Y. L.; Shen, J. L.; Hsu, I. J.; Cheng, P. W.; Cheng, C. F.; Ko, C.-H. *J. Non-Cryst. Solids* **2004**, *341*, 16.
(30) Feng, P. *Chem. Commun.* **2001**, 1668.
(31) Liao, Y. C.; Lin, C. H.; Wang, S. L. *J. Am. Chem. Soc.* **2005**, *127*, 9986.

It is well-known that different preparation processes can produce different kinds of defects.[12e] For the Pechini-type sol−gel derived Al_2O_3, we assume the luminescence band at 380−470 nm (which is the main contributor to the whole emission, diminished when the sample is annealed above 700 °C) must be related to some defects from the carbon impurities, since Al^{3+} itself cannot show luminescence. Considering the similar structure among Al_2O_3, SiO_2, and $Al_2O_3-SiO_2$, the most probable luminescent center is the radical carbonyl defects such as ≡Al−O−C•═O on the pore surface. We have the following evidence to support this conclusion. First, the profile of the emission spectrum (emission range 350−600 nm; λ_{max} = 386−430 nm) and the photoluminescence (PL) lifetimes (6.93, 5.82, and 5.64 ns) of our Pechini-type sol−gel derived Al_2O_3 are similar to those of C-SiO_2 gels (emission range 350−700 nm; λ_{max} varies between 405 and 550 nm depending on the preparation conditions; PL lifetimes <10 ns).[4] Second, carbon element has been detected by FT-IR spectra (Figure 1) and EDS in our Pechini-type sol−gel derived Al_2O_3 (Figure 3b). In order to check the effects of carbon impurity, we prepared Al_2O_3 through the solid-state reaction (SS) process (without using any organic solvents and additives, thus no carbon impurity involved). This SS-derived Al_2O_3 without carbon impurity did not show any luminescence under the same excitation condition (Figure 3b, blue line). From the above results, we can safely conclude that the luminescence peak at 430 nm in the Pechini-type sol−gel derived Al_2O_3 arises from the carbon impurities in the host lattice. In the preparation of Al_2O_3 via the Pechini-type sol−gel process, glycerol and PEG were employed as additives that contain large amounts of carbon. In the subsequent annealing process, most of the additives decomposed into H_2O and CO_2 and escaped from the system, but minor amounts of them may decompose to create a carbon interstitial defect, which is assumed to be the luminescent species in the lattice (like −O−Al−C−O−Al−O−). The bond energies of the Al−O, C−O, and C−C bonds are ∼512, ∼358, and ∼368 kJ/mol, respectively.[23,32] Note that the bond energy of Al−O is much larger than those of the C−O and C−C bonds and the bond energies lead to a significant dependence of the order of bond cleavage on the chemical and thermal environment.[15a] Therefore, the initial cleavage took place in the C−O bonds, which modified the intermolecular chemical environment and removed a portion of the network oxygen along with carbon. For example

$$\mathrm{Al{-}O{-}C{-}R} \rightarrow \mathrm{Al_2O_{3-}}_x + \mathrm{R^{\bullet}}x\mathrm{O} \quad (1)$$

$$\equiv\mathrm{Al{-}O{-}C{\downarrow}{-}O{-}Al}\equiv \rightarrow \equiv\mathrm{Al{-}O{-}C^{\bullet}} + {}^{\bullet}\mathrm{O{-}Al} \quad (2)$$

where x is the net oxygen vacancies created by the annealing process, and the vertical arrow shows the bond cleavage site. The above bond cleavages occur at a temperature where healing of the fragmented bonds and normalization of the coordination state are thermodynamically prohibited. Charge unbalances created at these sites must be rectified by localization of electrons and electron holes. The residual fragmented bonds are apparently the precursors for various centers. These defect centers include an electron being localized in a 2p orbital of the single-bonded carbon and the single-bonded oxygen. This would give rise to photoluminescence through a strong electron−photon coupling.[32−34]

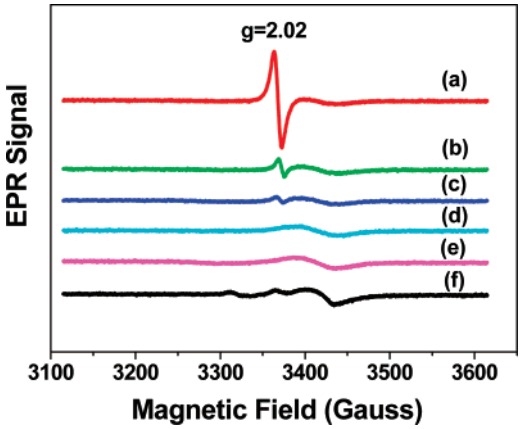

Figure 5. EPR curves for (a) AOSG500, (b) AOSG600, (c) AOSG700, (d) AOSG800, (e) AOSG900, and (f) AOSS500.

With raising the annealing temperature, the peak position of the PL band exhibits a blue shift. This can be explained as follows. With the increase of the temperature, the carbon defects decrease. Since the energy levels of carbon defects are located in the band gap of the alumina, the decrease of the carbon defects will induce the spacing of the energy levels of defects to become wide.[19] It will lead the PL band, which originated from electronic transitions between the energy levels of the carbon defects, to move toward the short wavelength (blue shift).

To prove the proposed assumption, EPR spectra for AOSG500, AOSG600, AOSG700, AOSG800, AOSG900, and AOSS500 samples were measured. Here we take the Al_2O_3 samples prepared by the solid-state reaction as the standard sample. The EPR signal is very weak for AOSS500 (Figure 5d), while AOSG500 exhibits a strong and sharp EPR band at g = 2.02 (Figure 5a). It can be seen clearly that with the increase of the annealing temperature, the EPR signal deceases. Moreover, the sharp EPR band cannot be seen in the EPR spectra for AOSG800 and AOSG900 samples, agreeing with the results of the emission spectra. This indicates that there indeed exist paramagnetic defects in Pechini-type sol−gel derived Al_2O_3. Since the EPR signal cannot be caused by Al^{3+} (no single electron in these ions), it must arise from some carbon-related defects, such as radical carbonyl defects.[5,12e]

In an ideal amorphous Al_2O_3, only Al−O bonds exist and it will not show any luminescence. The presence of structural defects will introduce electronic states into the band gap, resulting in luminescence of this material. As a summary,

(32) (a) Yoldas, B. E. *J. Mater. Res.* **1990**, *5*, 1157. (b) Yold, B. E. *J. Non-Cryst. Solids* **1992**, *147*, 614. (c) Hayakawa, T.; Hiramitsu, A.; Nogami, M. *Appl. Phys. Lett.* **2003**, *82*, 2975.
(33) (a) Weeks, R. A. *J. Appl. Phys.* **1986**, *27*, 1376. (c) Friebele, E. J.; Griscom, D. L.; Marrone, M. J. *J. Non-Cryst. Solids* **1985**, *71*, 133.
(34) (a) Jang, J.; Yoon, H. *Adv. Mater.* **2004**, *16*, 799. (b) Gimon-Kinsel, M. E.; Groothuis, K.; Balkus, K. J., Jr. *Microporous Mesoporous Mater.* **1998**, *20*, 67. (c) Lee, Y. C.; Liu, Y. L.; Shen, J. L.; Hsu, I. J.; Cheng, P. W.; Cheng, C. F.; Ko, C. H. *J. Non-Cryst. Solids* **2004**, *341*, 16.

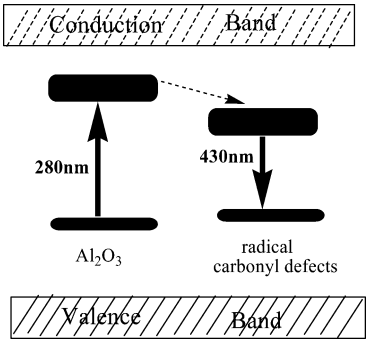

Figure 6. Energy band diagram showing the possible defects and emission process in Pechini-type sol−gel derived Al_2O_3.

the whole emission process in our Pechini-type sol−gel derived Al_2O_3 is schematically shown in Figure 6.

In order to further confirm the proposed mechanism, the electronic structures of the amorphous Al_2O_3 and defective amorphous Al_2O_3 were calculated. The atomic structure of amorphous alumina was built using molecular dynamics (MD) according to refs 35 and 36. It has been reported that the coordination number of Al atom in amorphous Al_2O_3 has a value between 4.1 and 4.8.[22] Therefore, MD was carried out for a microcanonical ensemble (NVE) of $N = 160$ atoms taken in a $(2 \times 2 \times 1)$ supercell of orthorhombic primitive unit cells ($a = 0.484$ nm, $b = 0.833$ nm, $c = 0.895$ nm) of κ-Al_2O_3.[37] All the MD presented here was performed using GULP code.[38] The three-body and two-body potentials suggested by Blonski and Garofalini were employed in the calculations, which have previously been shown to provide good descriptions of the silica−alumina interface and of silica glasses.[39,40] First, the liquid phase of alumina was simulated at the temperature of 4000 K, which is much higher than the melting temperature of Al_2O_3. The liquid phase was equilibrated during 4000 time steps, where a time step was taken as $\Delta t = 0.5$ fs. Amorphous Al_2O_3 was then obtained by simulated quenching of the liquid alumina at 300 K. The cooling rate of this simulated quenching was 5×10^{13} K s^{-1}, and the total simulating time for quenching was 74 ps. The obtained atomic structure of amorphous alumina is shown in Figure 7a.

The electronic structure of amorphous alumina and defective amorphous alumina using CASTEP code based on the density functional theory (DFT), and exchange and correlation have been treated by the generalized gradient approximation (GGA) within the scheme due to Perdew−Burke−Ernzerhof (PBE).[41,42] This method has been applied

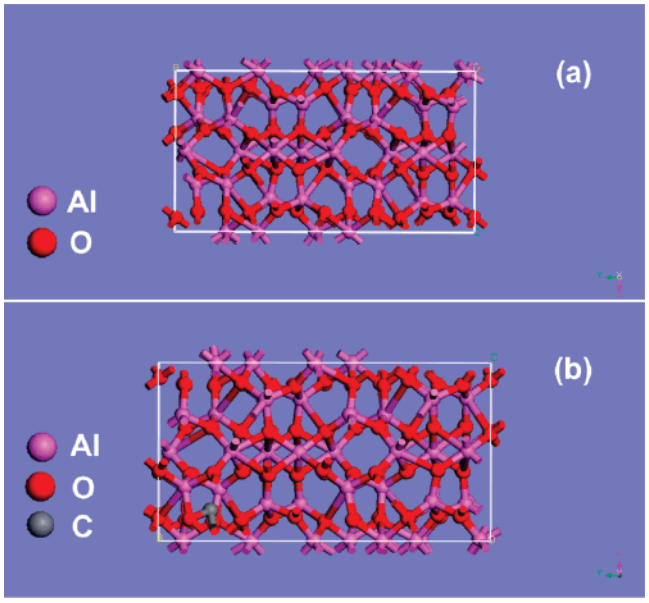

Figure 7. (a) Amorphous structure of Al_2O_3 (produced by simulated quenching); (b) model structure of defective amorphous Al_2O_3.

to many materials, such as amorphous ice, amorphous silicon, amorphous indium phosphide, and so forth.[43−48] In this calculation, the structural model of defective amorphous alumina was established containing 161 atoms as a superlattice with constant volume and under periodic boundary conditions (Figure 7b). The calculated band structures of amorphous alumina and defective amorphous alumina are given in parts a and b, respectively, of Figure 8. It can be seen that the calculated band gap for amorphous alumina is larger than that of defective amorphous alumina, confirming the trend of the model proposed in the luminescent mechanisms. The energy levels of defective amorphous alumina are located close to the Fermi level (determined by the calculated partial density of state (DOS) plots, Figure 9) and are ascribed to the energy levels of C(2p). From Figure 9, it can be seen clearly that these levels (~ -0.04 eV, ~ 1.9 eV) are between the Al(3s) levels in the conduction band (~ 4.2 eV) and O(2p) levels in the valence band (~ -5.8 eV). This indicates that the wavelength of the white emission arises from the carbon-induced defects, agreeing well with the results of spectra analysis and the proposed luminescent mechanism. It should be noted that the calculated band gaps in semiconductors may be underestimated using this first-principles energy band calculation, probably due to many factors such as the action of the crystal field, the structure model, the defect density, the limits of method itself, and so

(35) (a) Chang, H.; Choi, Y.; Kong, K.; Ryu, B. H. *Chem. Phys. Lett.* **2004**, *391*, 293. (b) Gutiérrez, G.; Johansson, B. *Phys. Rev. B* **2002**, *65*, 104202. (c) Lampartner, P.; Kniep, R. *Physica B* **1997**, *234−236*, 405.
(36) (a) San Miguel, M. A.; Sanz, J. F.; Alvarez, L. J.; Odriozola, J. A. *Phys. Rev. B* **1998**, *58*, 2369. (b) Hemmati, M.; Wilson, M.; Madden, P. A. *J. Phys. Chem. B* **1999**, *103*, 4023. (c) Sakurai, Y. *J. Non-Cryst. Solids* **2000**, *271*, 218.
(37) Ollivier, B.; Retoux, R.; Lacorre, P.; Massiot, D.; Férey, G. *J. Mater. Chem.* **1997**, *7*, 1049.
(38) Gale, J. D. *J. Chem. Soc., Faraday Trans.* **1997**, *93*, 629.
(39) Blonski, S.; Garofalini, S. H. *J. Am. Ceram. Soc.* **1997**, *80*, 1997.
(40) Blonski, S.; Garofalini, S. H. *J. Phys. Chem.* **1996**, *100*, 2201.
(41) Segall, M. D.; Lindan, P. L. D.; Probert, M. J.; Pickard, C. J.; Hasnip, P. J.; Clark, S. J.; Payne, M. C. *J. Phys.: Condens. Mater.* **2002**, *14*, 2717.
(42) Perdew, J. P.; Ernzerhof, B. M. *Phys. Rev. Lett.* **1996**, *77*, 3865.
(43) He, C.; Lian, J. S.; Jiang, Q. *J. Phys. Chem. B* **2005**, *109*, 19893.
(44) Kim, S. K.; Kim, Y.; Hong, J.; Tanaka, I.; No, K. *J. Appl. Phys.* **2005**, *97*, 073519.
(45) (a) Zheng, B.; Zheng, W. T.; Zhang, K.; Wen, Q. B.; Zhu, J. Q.; Meng, S. H.; He, X. D.; Han, J. C. *Carbon* **1999**, *263*, 442. (b) Zheng, B.; Zheng, W. T.; Zhang, K.; Wen, Q. B.; Zhu, J. Q.; Meng, S. H.; He, X. D.; Han, J. C. *Carbon* **2006**, *44*, 962. (c) Zheng, B.; Zheng, W. T.; Yu, S. S.; Tian, H. W.; Meng, F. L.; Wang, Y. M.; Zhu, J. Q.; Meng, S. H.; He, X. D.; Han, J. C. *Carbon* **2005**, *43*, 1976.
(46) Koslowski, T.; Kob, W.; Vollmayr, K. *Phys. Rev. B* **1997**, *56*, 9469.
(47) Lewis, L. J.; Vita, A. D. *Phys. Rev. B* **1998**, *57*, 1594.
(48) Hayakawa, Y.; Kohiki, S.; Arai, M.; Yoshikawa, H.; Fukushima, S.; Wagastsuma, K.; Oku, M.; Shoji, F. *Phys. Rev. B* **1999**, *59*, 11125.

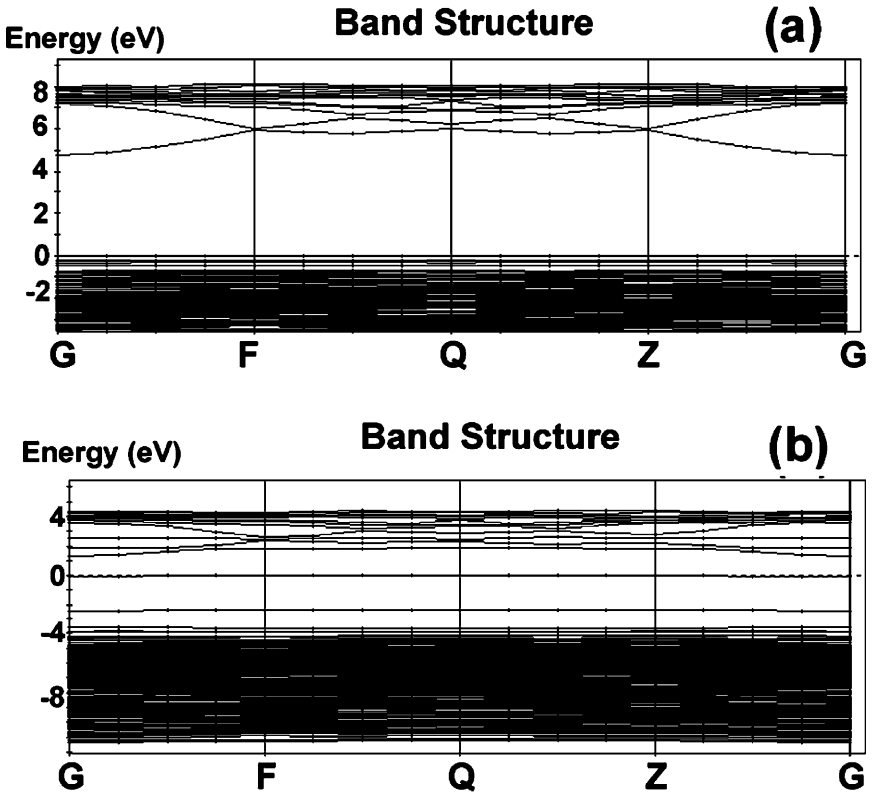

Figure 8. Calculated band structures according to the model of Figure 7: (a) amorphous Al_2O_3 and (b) defective amorphous Al_2O_3.

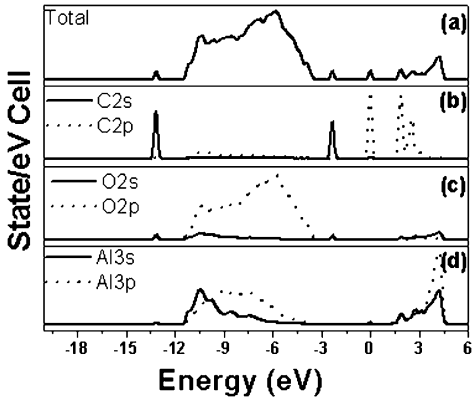

Figure 9. Calculated DOS of defective amorphous Al_2O_3.

forth. [49] These factors are expected to give some contributions to the change of the calculated energy level, but were not included due to the difficulty of doing so correctly. Nevertheless, the results of the calculation can well explain the luminescence phenomenon and the proposed mechanism. Here, we can only say that the Pechini-type sol−gel derived amorphous Al_2O_3 samples show the mentioned luminescence properties and the emission intensities can be controlled by the annealing temperature. It is expected that the luminescence properties (emission color and intensity) can be further tuned by controlling the concentration of PEG, adding some nontoxic inorganic ions (Li^+, Na^+, K^+, etc.), and so on. This will be done in other systems (such as BPO_4) and reported in the near future.

(49) Fu, Z. L.; Zhou, S. H.; Zhang, S. Y. *J. Solid State Chem.* **2005**, *178*, 230.

IV. Conclusions

Amorphous Al_2O_3 powder samples have been successfully prepared via the Pechini-type sol−gel process. The Pechini-type sol−gel derived amorphous Al_2O_3 annealed at 500 and 600 °C exhibits white emission centered at 430 nm and bright bluish-white emission centered at 407 nm, respectively. The results of FT-IR and EDS characterizations indicates that the carbon impurity has not been removed completely in the Pechini-type sol−gel derived samples due to the relatively low annealing temperatures. The EPR spectra confirm that there exist paramagnetic defects in amorphous Al_2O_3. From the results it can be concluded that the luminescence of the amorphous Al_2O_3 powders is from the carbon-related defects such as radical carbonyl defects. The DFT calculation of the defective amorphous Al_2O_3 further proves that the bluish-white emission arises from the carbon-related impurities (defects), agreeing well with the results of spectral analysis and the proposed luminescent mechanisms.

Acknowledgment. This project is financially supported by the foundation of "Bairen Jihua" of the Chinese Academy of Sciences, the National Natural Science Foundation of China (50572103 and 20431030), and the MOST of China (Nos. 2003CB314707 and 2007CB935502).

Supporting Information Available: XRD patterns of Al_2O_3 prepared by Pechini-type sol−gel process (SG) and solid-state reaction (SS) of (a) AOSS500, (b) AOSG500, (c) AOSG600, (d) AOSG700, (e) AOSG800, and (f) AOSG900. (Figure S1). This material is available free of charge via the Internet at http://pubs.acs.org.

IC700652V